Inorg. Chem. **2002**, *41*, 931–937

SrInGe and EuInGe: New Zintl Phases with an Unusual Anionic Network Derived from the $ThSi_2$ Structure

Jiang-Gao Mao, Joanna Goodey, and Arnold M. Guloy*

Department of Chemistry and the Texas Center for Superconductivity, University of Houston, Houston, Texas 77204-5641

Received March 16, 2001

Two new isostructural Zintl phases, EuInGe and SrInGe, are obtained from high-temperature reactions of the pure elements in welded Ta tubes. Both ternary phases crystallize in a new structure type in space group *Pnma* (No. 62), with $a = 4.921(1)$ Å, $b = 3.9865(9)$ Å, and $c = 16.004(3)$ Å for EuInGe; and $a = 5.021(1)$ Å, $b = 4.0455(9)$ Å, and $c = 16.188(4)$ Å for SrInGe. The crystal structures established by single-crystal X-ray diffraction feature zigzag chains of 3-bonded Ge atoms and puckered layers of 4-bonded In atoms. The two structural units are linked into an anionic network with channels composed of 5-membered and 7-membered rings. The channels are filled by the respective divalent cations. The chemical bonding of the anionic $[InGe]^{2-}$ network, derived from a one-electron oxidative distortion of the α-$ThSi_2$ structure, is explained using extended-Hückel band structure calculations. Magnetic measurements indicate that EuInGe exhibits Curie–Weiss paramagnetic behavior above 35 K and antiferromagnetic behavior below 35 K. The calculated effective moment, $\mu_{eff} = 8.11\ \mu_B$, of EuInGe and the diamagnetic behavior of SrInGe are consistent with the oxidation states of Eu(II) and Sr(II), respectively.

Introduction

The development of new solid state materials requires an increased understanding of stoichiometry−structure−property relationships. Among the empirical concepts that relate stoichiometry with structure and properties, the Zintl−Klemm concept has been successfully applied to a wide range of main-group-element polar intermetallics.[1] However, its application to less polar intermetallics has been inconsistent. Our current research on polar intermetallic phases formed between the elements of groups 13 and 14 with one or more of the electropositive alkali or alkaline earth metals has been motivated by the need to understand the limits of the Zintl−Klemm concept.[2] Failure of the concept applies mostly in compounds that involve group 13 elements (trielides), where up to 5 electrons per atom must be accommodated to satisfy the Zintl picture. It seems unlikely that these elements have a sufficiently high effective core potential to accumulate significant electron density without significant mixing with the electronic states of the metal component. In addition, group 13 elements and their compounds often do not conform to classical chemical bonding concepts. Thus, an empirical boundary between group 13 and 14 elements signifies the limits of the Zintl concept as applied to polar intermetallics. Many violations are also observed among polar intermetallics containing group 14 and 15 elements that imply that the Zintl boundary is not absolute. In the spectrum from intermetallic compounds to Zintl or valence compounds to insulators, we observe a smooth transition in their chemical bonding going from metallic to ionic.[3] At the border between Zintl phases and normal intermetallics, typical properties of Zintl phases diminish and metallic conductivity appears. Thus, the Zintl border provides a fertile area to search for materials with novel electronic properties and offers unique opportunities in investigating relationships between crystal structure, chemical bonding, and physical properties.

Binary AB_2 and ternary ABC compounds of electropositive metals (alkaline earth or rare earth metals) with triels and tetrels generally exhibit crystal structures that feature anionic networks of 3-connected and/or 4-connected trielide and tetrelide atoms.[4,5] Our exploratory work was initially

* Author to whom correspondence should be addressed. E-mail: aguloy@uh.edu.

(1) Von Schnering, H. G. *Angew. Chem., Int. Ed. Engl.* **1981**, *20*, 33. Schäfer, H. *Annu. Rev. Mater. Sci.* **1985**, *15*, 1.
(2) Corbett, J. D. In *Chemistry, Structure and Bonding of Zintl Phases and Ions*; Kauzlarich, S., Ed.; VCH Publishers: New York, 1996; p 139.
(3) Miller, G. In *Chemistry, Structure and Bonding of Zintl Phases and Ions*; Kauzlarich, S., Ed.; VCH Publishers: New York, 1996; pp 1−55. Nesper, R. *Angew. Chem., Int. Ed. Engl.* **1991**, *30*, 789.
(4) Pöttgen, R.; Hoffmann, R. D. *Z. Kristallogr.* **2001**, *216*, 127.
(5) Villars, P.; Calvert, L. D. *Pearson's Handbook of Crystallographic Data for Intermetallic Phases*, 2nd ed.; American Society for Metals International: Metals Park, OH, 1991.

10.1021/ic0102891 CCC: $22.00
Published on Web 01/18/2002

motivated by the desire to understand the stability of 3-connected and 4-connected layered networks with varying electron counts as it pertains to the problem associated with the layered CaGaGe structure.[6] The 3-connected networks may be planar, as in the graphitic layers of the AlB_2 type, and exhibit extended π-conjugation.[7,8] This structure is exhibited by the binary trielides, such as MgB_2 and $CaGa_2$. The significance of these chemical systems has been emphasized by the recent discovery of high-temperature superconductivity in the nominal Zintl phase MgB_2.[9] The anionic layers of the binary tetrelides, $CaSi_2$ and $CaGe_2$, and their isoelectronic derivatives exhibit 3-connected puckered nets as in α-As. The "buckling" of the hexagonal nets in $CaGe_2$, as well as in other more complex anionic covalent structures, can be attributed to the onset of a stereochemically active lone pair.[8,10] The structures of related complex ternaries, in particular, those of the isostructural compounds CaGaGe and CaInGe which feature anionic double layers are composed of 3-bonded Ge as in $CaGe_2$ and 4-bonded Ga or In atoms, as in $CaIn_2$.[6,11] Other distortion modes of the planar 3-connected nets in AlB_2 compounds have been reported and discussed in terms of the transformation of a delocalized π-bonding to localized bonds between layers as in $CaIn_2$, $BaIn_2$, LiGaGe, and $CaAl_2Si_2$.[2,3,6−8,11−12]

Among the ubiquitous crystal structures exhibited by AB_2 intermetallics, the $ThSi_2$ structure type represents a typical structure exhibited by polar intermetallics that usually do not conform to the Zintl concept.[5,7] Many compounds that crystallize with this structure type (e.g., rare earth metal disilicides and digermanides) have generated research interest due to their novel physical properties, such as superconductivity and unusual magnetic ordering.[13] Theoretical investigations on the metallic structure type reveal that it is stabilized by electron counts higher than the 3-bonded conjugated nature of the anions would imply.[7] The theoretical studies also indicate that when the π^*-states of the anionic framework are sufficiently populated, the $ThSi_2$ structure is stabilized with respect to other 3-bonded networks such as the hexagonal graphitic layers in AlB_2-type and the puckered layers in the $CaSi_2$-type and related structures.

Many binary and ternary phases formed between elements of group 14, with alkaline earth or rare earth metals crystallize in the $ThSi_2$ structure type or its disordered variants.[5] Despite the prevalence of the high-density structure type among polar intermetallics, there have been just a few valence compounds or Zintl phases that exhibit this structure. Examples include the high-pressure form of $BaGe_2$ and the ternary LaAlGe.[13] It was pointed out by Zheng and Hoffmann that a unique interaction exists between the non-neighbor atoms of parallel chains in the anionic network of the $ThSi_2$ structure type.[7] The significance of the interaction as a possible route to the formation of σ-bonds between neighboring parallel chains was thereby implied. However, the bond formation was alluded to occur only for carbon analogues since the relevant interchain distances for disilicides and digermanides were said to be too large for the specified interaction to be observed. Moreover, a corresponding structure derived from such a distortion of the anionic silicide net in $ThSi_2$ was largely unknown. Herein we report the preparation and characterization of new Zintl phases that represent an unprecedented distorted variant of the $ThSi_2$ structure. The title compounds EuInGe (**1**) and SrInGe (**2**) exhibit a structure derived from the $ThSi_2$ structure with neighboring chains linked by σ-bonds as previously suggested.

Experimental Section

Syntheses. The title compounds were synthesized in high yields through high-temperature reactions of the pure elements (Eu and Sr pure metals from Aldrich; In shots, 99.9999%; Ge pieces, 99.9999%) according to molar ratio of 1:1:1 in welded Ta tubes within an evacuated quartz jacket. The reactions were performed at 810 and 850 °C for Eu and Sr compounds, respectively, for 7 days with prior heating under dynamic vacuum at 300 °C for 1 day. Afterward the reaction mixtures were allowed to cool very slowly (0.1 °C/min) to room temperature. All sample manipulations were done within a purified argon atmosphere glovebox. All lines in the X-ray powder diffraction patterns could be indexed according to those calculated on the basis of single-crystal structure refinements.

Crystal Structure Determination. Bricklike black single crystals were optically selected and sealed within thin-walled glass capillaries under argon atmosphere. Selected single crystals were mounted on a Siemens Smart 1K CCD (Mo Kα radiation, graphite monochromator) at 293(2) K. A hemisphere of data (1271 frames at 5 cm detector distances) for each compound was collected by narrow-frame method with scan widths of 0.30° in ω and exposure time of 35 s per frame. The first 50 frames were recollected in the end of data collection to monitor the stability of the crystal, and it was found that the decay in intensity was negligible. The data were corrected for Lorentz factor, polarization, air absorption, and absorption due to variations in the path length through the detector faceplate. Absorption corrections, based on the ψ-scan method, were also applied. Superstructure peaks associated with larger lattice parameters and/or lower symmetry, using a systematic narrow-frame method with longer exposure times (60−80 s per frame), were not observed.

Based on observed systematic absences, the space group was uniquely determined to be *Pnma* (No. 62) or $Pn2_1a$ (No. 33). The centrosymmetric space group *Pnma* was initially used for structural solution and later confirmed by subsequent refinements. Both structures were solved by direct methods that revealed the positions of all atoms. Refinements were performed using least-squares methods on the atomic coordinates and anisotropic thermal parameters.[14] During isotropic refinement for both compounds, it was observed that the thermal parameters of the indium atoms located on a site with *m* symmetry (4c position) were anomalously large. Furthermore, the refinement was largely unsatisfactory

(6) Xu, Z. Ph.D. Thesis, University of Houston, 1999.
(7) Zheng, C.; Hoffmann, R. *Inorg. Chem.* **1989**, *28*, 1074.
(8) Burdett, J. K.; Miller, G. J. *Chem. Mater* **1990**, *2*, 12.
(9) Nagamatsu, J.; Nakagawa, N., Muranaka, T.; Zenitani, Y.; Akimitsu, J. *Nature* **2001**, *410*, 63.
(10) Yoshizawa, K.; Yumura, T.; Yamabe, T. *J. Chem. Phys.* **1999**, *110*, 11534.
(11) (a) Bruzzone, G.; Ruggiero, A. F., *J. Less-Common Met.* **1964**, *7*, 368. (b) Bockelmann, W.; Schuster, H.-S. *Z. Anorg. Allg. Chem.* **1974**, *410*, 233.
(12) Ramirez, R.; Nesper, R.; von Schnering, H. G. *Z. Naturforsch.* **1987**, *42a*, 670.
(13) (a) Evers, J.; Oehlinger, G.; Weiss, A. *Z. Naturforsch., B: Anorg. Chem., Org. Chem.* **1980**, *35B*, 397. (b) Guloy, A. M.; Corbett, J. D. *Inorg. Chem.* **1991**, *30*, 4789.

Table 1. Crystal Data and Structure Refinements for Compounds **1** and **2**[a]

compound	**1**	**2**
formula	EuInGe	SrInGe
fw	339.37	275.03
temp (K)	298	298
cryst syst	orthorhombic	orthorhombic
space group	*Pnma* (No. 62)	*Pnma* (No. 62)
a/Å	4.921(1)	5.021(1)
b/Å	3.9865(9)	4.0455(9)
c/Å	16.004(3)	16.188(4)
vol/ Å^3	314.0(1)	328.8(1)
Z	4	4
ρ_{calcd} (g cm^{-3})	7.179	5.555
μ (mm^{-1})	36.193	31.882
GOF	1.009	1.069
R1/wR2 ($I > 2\sigma(I)$)	0.0207/0.0392	0.0396/0.0738
R1/wR2 (all data)	0.0345/0.0419	0.0643/0.0797

[a] GOF $= [\sum(w(F_o^2 - F_c^2)^2)/(n-p)]^{1/2}$. R1 $= (\sum||F_o| - |F_c||)/(\sum|F_o|)$. wR2 $= [\sum w(|F_o| - |F_c|)^2/\sum w|F_o|^2]^{1/2}$.

marked with relatively high residuals (R1 > 10% (for **1**), 9% (for **2**)), and large electron density residuals (~19−20 e Å^{-3}) around the indium sites. Anisotropic refinement did not improve the refinement and also resulted in abnormal cigar-shaped indium thermal ellipsoids ($U_{22} \sim 0.30$ Å^2). The anomalous thermal parameter was not resolved by subsequent refinement of the indium occupancy parameters. All these symptoms indicated a crystallographic disorder associated with the indium atom. Consequently, indium atoms in both compounds were refined using disorder models based on displacing the indium atoms from the *m* (4c) position. Thus, indium atoms were refined at general positions that are 0.4085 Å (for **1**) and 0.4075 Å (for **2**), respectively, away from the ideal *m* (4c) sites. Thus, the resulting indium position can crystallographically be described as a "split atom" position, with site occupancy factors reduced and subsequently refined to 50%. The "split atom" model was supported by careful analysis of the Fourier and difference maps around the indium atoms. The resolution of the disorder problem, using the "split atom" model, resulted in much improved structure refinements with R1 values significantly lower, 2.07% for **1** and 3.96% for **2**. Moreover, the resulting thermal parameters of indium became well-behaved and the final difference maps showed residuals that were essentially featureless (1.055 e Å^{-3} for **1**, and 1.413 e Å^{-3} for **2**; these residuals are less than 1.0 Å from the cations). Attempts to resolve the disorder of the indium atoms in the noncentrosymmetric space group $Pn2_1a$ were also unsuccessful. The possibility of twinning was discounted inasmuch as identical lattice parameters and refinement results were obtained from several single crystals. Moreover, the observed disorder in the resulting structure is not uncommon in solid state materials. The data collection and refinement parameters are summarized in Table 1. The atomic coordinates and equivalent thermal parameters and important bond lengths and angles are listed in Tables 2 and 3, respectively. More details on the crystallographic studies as well as anisotropic thermal parameters are given in the Supporting Information. A full list of observed and calculated structure factors is available from A.M.G.

The chemical compositions of a number of single crystals were quantitatively analyzed by microprobe, WDS (wavelength dispersive spectrometer) techniques. Results indicated uniform compositions corresponding to EuInGe and SrInGe that are in excellent agreement with the results from both single-crystal structure refinements. The chemical compositions of **1** and **2** were also confirmed by the high-yield (>95%) synthesis of both compounds from the high-temperature stoichiometric reactions of the pure elements. Accurate lattice parameters were obtained by careful indexing of the experimental X-ray diffraction patterns with the theoretical diffraction pattern obtained from the single-crystal structure refinement results, using NBS Si as an internal standard.

Table 2. Atomic Coordinates and Equivalent Isotropic Displacement Parameters (Å^2) for Compounds **1** and **2**

atom	*x*	*y*	*z*	*U*(eq)[a]
		EuInGe		
Eu(1)	0.0193(1)	0.2500	0.3925(1)	0.012(1)
In(1)	0.5024(2)	0.1476(2)	0.7104(1)	0.012(1)
Ge(1)	0.4236(2)	0.2500	0.5422(1)	0.011(1)
		SrInGe		
Sr(1)	0.0199(2)	0.2500	0.3918(1)	0.013(1)
In(1)	0.5031(2)	0.1493(2)	0.7100(1)	0.013(1)
Ge(1)	0.4229(2)	0.2500	0.5420(1)	0.011(1)

[a] *U*(eq) is defined as one-third of the trace of the orthogonalized $\mathbf{U}_{ij}$ tensor. The In(1) atoms in both EuInGe and SrInGe are disordered over two mirror-plane related positions, and hence their occupancies were reduced and refined to 50%.

Table 3. Selected Bond Lengths (Å) and Angles (deg) for EuInGe and SrInGe

EuInGe			SrInGe		
Eu(1)−Ge(1)		3.115(1)	Sr(1)−Ge(1)		3.162(2)
Eu(1)−Ge(1)	×2	3.1334(9)	Sr(1)−Ge(1)	×2	3.191(1)
Eu(1)−In(1)	×2	3.281(1)	Sr(1)−In(1)	×2	3.326(2)
Eu(1)−In(1)	×2	3.319(1)	Sr(1)−In(1)	×2	3.359(2)
Eu(1)−In(1)	×2	3.438(1)	Sr(1)−In(1)	×2	3.496(2)
Eu(1)−Ge(1)	×2	3.547(1)	Sr(1)−Ge(1)	×2	3.615(1)
Eu(1)−In(1)		3.744(1)	Sr(1)−In(1)		3.790(1)
In(1)−Ge(1)		2.751(1)	In(1)−Ge(1)		2.780(2)
In(1)−In(1)	×2	2.8857(9)	In(1)−In(1)	×2	2.940(1)
In(1)−In(1)		3.170(2)	In(1)−In(1)		3.230(2)
Ge(1)−Ge(1)	×2	2.522(1)	Ge(1)−Ge(1)	×2	2.557(2)
Ge(1)−In(1)−In(1)		120.53(4)	Ge(1)−In(1)−In(1)		120.92(6)
Ge(1)−In(1)−In(1)		105.52(4)	Ge(1)−In(1)−In(1)		105.45(5)
In(1)−In(1)−In(1)		117.01(5)	In(1)−In(1)−In(1)		117.30(8)
Ge(1)−In(1)−In(1)		98.54(2)	Ge(1)−In(1)−In(1)		98.43(2)
In(1)−In(1)−In(1)	×2	106.44(3)	In(1)−In(1)−In(1)	×2	106.10(4)
Ge(1)−Ge(1)−Ge(1)		104.42(7)	Ge(1)−Ge(1)−Ge(1)		104.59(9)

Band Calculations and Property Measurements. Consistent with the premise of the Zintl concept, the electropositive metals Eu and Sr were assumed to donate their respective valence electrons to the anionic $[InGe]^{2-}$ networks in **1** and **2**. The electronic band structure calculations on the three-dimensional anionic network in both compounds were carried out using the extended Hückel method.[15,16] The following parameters were used for the Slater-type wave functions representing valence orbitals of indium (In, *Hii* (eV), −12.60 (5s), −6.19 (5p); ζ_1, 1.903 (5s), 1.677 (5p)) and germanium (Ge, *Hii* (eV), −16.0 (4s), −9.0 (4p); ζ_1, 2.16 (4s), 1.85 (4p)). The atomic parameters *Hii* and ζ, the orbital and Slater exponents, respectively, were taken from literature values.[17,18] A sufficiently large set of 70 k-points, selected from an irreducible wedge of the orthorhombic Brillouin zone, was used in all calculations and integrations for Mulliken populations, overlap populations, total energies, densities of states (DOS), and crystal orbital overlap populations (COOP) curves.

Magnetic susceptibility measurements were performed using an Oxford Instruments Maglab 9T vibrating sample magnetometer

(14) Sheldrick, G. M. *SHELXTL*, version 5.03; Siemens Analytical X-ray Instruments: Madison, WI, 1995. Sheldrick, G. M. *SHELX-96 Program for Crystal Structure Determination*; 1996.

(15) Hoffmann, R. *J. Chem. Phys.* **1963**, *39*, 1397.
(16) Whangbo, M.-H.; Hoffmann, R. *J. Am. Chem. Soc.* **1978**, *100*, 6093.
(17) (a) Xu, Z.; Guloy, A. M. *J. Am. Chem. Soc.* **1997**, *119*, 10541. (b) Janiak, C.; Hoffmann, R. *J. Am. Chem. Soc.* **1990**, *112*, 5924.
(18) Xu, Z.; Guloy, A. M. *J. Am. Chem. Soc.* **1998**, *120*, 7349.

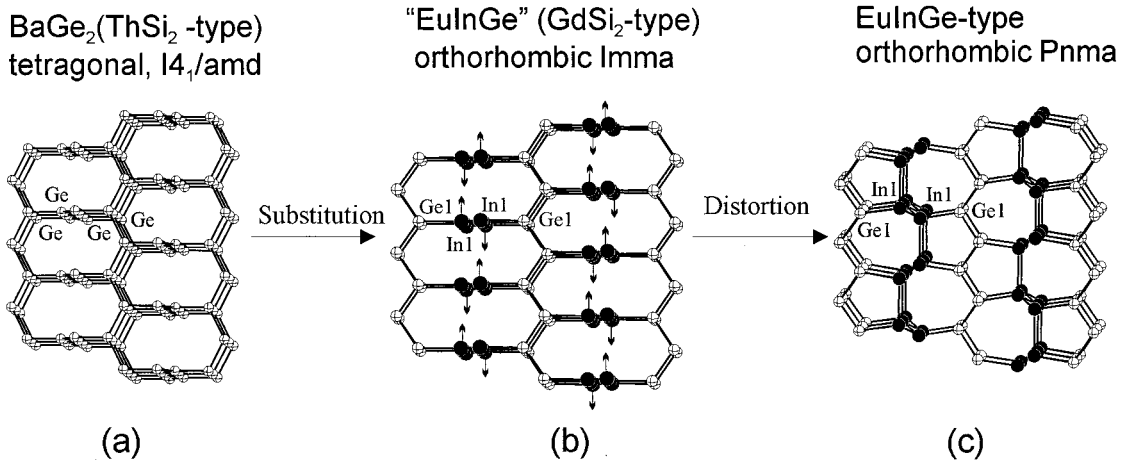

Figure 1. Diagram showing the structural relationship between (a) $BaGe_2$ ($ThSi_2$ structure type), (b) hypothetical EuInGe with $GdSi_2$ type, and (c) "disordered model" EuInGe. The small arrows indicate one possible displacement indium atoms may adapt.

(VSM). The susceptibility measurements were made on single-phase pressed powder samples over the temperature range 4−300 K, at magnetic field strengths of 0.1 to 1.0 T. Each of the polycrystalline powder samples was pressed into $^1/_8$ in. diameter pellets that were fastened to a standard sample holder with Teflon tape. All manipulations and handling of samples were performed under argon atmosphere to avoid oxidation of the air-sensitive compounds. The magnetic susceptibility data were initially corrected for diamagnetic contributions from the sample holder and ion cores.

Results and Discussion

The general structural features of the $ThSi_2$ structure are two independent slabs of parallel zigzag chains, with the chains from one type of slab oriented orthogonal to the chains of the other slab. These slabs are stacked alternately, and the atoms in each chain are alternately connected to the adjoining layers. The resulting three-dimensional anionic network consists of 3-bonded Si atoms that are in full conjugation with only two neighbors (See Figure 1a). It was suggested that a new type of interaction may arise from a σ-overlap between π-orbitals of nearest-neighbor atoms of parallel chains.[7] However, this interaction was deemed weak in isostructural compounds formed by larger post-transition atoms due to the long interchain distances.

The isostructural Zintl phases, **1** and **2**, represent a new structure type in Zintl and intermetallic chemistry. Both compounds crystallize in an orthorhombic structure (space group *Pnma*) that can be derived from the distortion of the tetragonal (space group $I4_1/amd$) $ThSi_2$ type in a manner similar to that alluded to by Zheng and Hoffmann.[7] The relationships between the high-pressure $BaGe_2$, with the $ThSi_2$ structure type, and the EuInGe structures are illustrated in Figure 1. First, the high-symmetry tetragonal structure of $BaGe_2$ (hp) is lowered to an orthorhombic derivative through an ordered substitution of the germanium sites. The ordered substitution effectively differentiates the two types of zigzag chains in the hp-$BaGe_2$ and the $ThSi_2$ structure type. The "broken" symmetry relationship is exhibited between compounds that exhibit the tetragonal ($I4_1/amd$) $ThSi_2$ and the orthorhombic (*Imma*) $GdSi_{2-x}$ structure types. In many nonstoichiometric disilicides and digermanides, the observed dimorphism has been described as a second-order phase transition controlled by the unequal distribution of vacancies within the orthogonal zigzag chains.[13b] The ordered substitution of indium atoms in EuInGe and the concomitant dissimilarity of the intra- and interchain lengths, as well as the slight "tilting" of the germanium chains with respect to the pseudotetragonal axis, further remove the body-centering element (*I*) and lowers the space group symmetry to *Pmna*. The refined anionic substructure of **1** and **2**, with the indium positions at the *m* (4c) site of the space group *Pnma*, is illustrated in Figure 1b. The idealized model contains distinct all-In and all-Ge zigzag chains that run perpendicular to each other. The shortest In−In distances between parallel indium chains in the idealized (no-disorder) structure are 3.987(1) and 4.046(1) Å for **1** and **2**, respectively. The anomalous thermal parameter of indium when placed on the *m* site and the subsequent resolution by the "split atom" model indicates that the indium chain is disordered over a mirror plane that contains the zigzag chain axis. The disorder model indicates a "buckling" of the indium chain that effectively displaces the indium atoms from the mirror plane (randomly in opposite directions) and results in shorter In−In interchain distances (3.170(2) and 3.230(2) Å in **1** and **2**, respectively). Thus, the crystal structure of EuInGe, as shown in Figure 1c, can be viewed as being derived from the ordered substitution and distortion of the 3-connected network in tetragonal high-pressure form $BaGe_2$ (α-$ThSi_2$ type).

It is important to note that the lowering of the symmetry of the $ThSi_2$ can also be achieved in another fashion, as in LaAlGe.[13b] The ordered substitution of Al in the $LaGe_{2-x}$ phases results in the LaPtSi structure ($I4_1md$) that features every Al bonded to three Ge atoms, and each Ge is bonded to three Al atoms. This effectively maintains the symmetry equivalence of the [AlGe] chains and preserves the tetragonal symmetry. Using group−subgroup relationships and group analyses,[19] further lowering of the symmetry to the orthorhombic space group *Fddd* has been predicted, but a related orthorhombic structure has not yet been reported.[13b]

The unit cell parameters of **1** and **2** are related to hp-$BaGe_2$ ($ThSi_2$ type) in the following manner: $a_{EuInGe} \approx a_{BaGe2}$, b_{EuInGe}

(19) Pöttgen, R.; Johrendt, D. *Chem. Mater.* **2001**, *12*, 875.

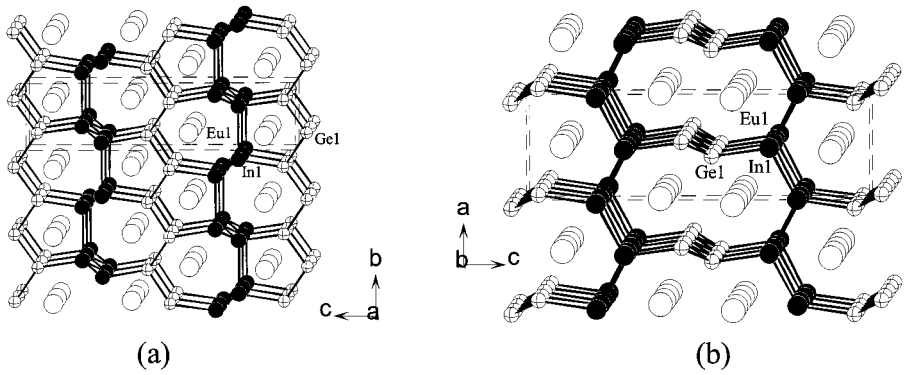

Figure 2. (a) A ⟨100⟩ view of the crystal structure of EuInGe. Europium, indium, and germanium atoms are represented as large (empty), medium (solid), and small (crossed) spheres, respectively. (b) A ⟨010⟩ view of the crystal structure of EuInGe. Relevant distances are listed as follows: In1−In1 2.8857(9), In1−In1 3.170(2), In1−Ge1 2.751(1), and Ge1−Ge1 2.552(1) Å.

$\approx b_{BaGe2}$, and $c_{EuInGe} \approx c_{BaGe2}$. The "distortion" of the 3-connected network in **1** and **2** can be described in terms of the joining of one type of parallel zigzag chains through In−In bonds. Thus, the 3-connected network is formally transformed to a network of 4-bonded In and 3-bonded Ge atoms. The "distortion" of the structure of **1** and **2** from the $ThSi_2$ type mainly occurs along the *b* direction. This is manifested by the observed lengths of the *b*-axis that are significantly shorter in **1** and **2** than those in hp-$BaGe_2$ (4.755 Å) and the related LaAlGe (4.336(1) Å). Moreover, the unit cell of EuInGe is slightly smaller than that of SrInGe, and so are the corresponding In−In and In−Ge bond lengths. Careful examination of the crystal structures of **1** and **2** indicates that disordered indium atoms exhibit a geometry close to tetrahedral, as shown in Figure 2a. Thus, each indium atom is 4-bonded to three neighboring In atoms and one Ge atom. There are two types of In−In distances in **1** and **2**: (a) the shorter intrachain (2.8857(9) Å for **1** and 2.940(1) Å for **2**), and (b) longer interchain distances (3.170(2) Å for **1** and 3.230(2) Å for **2**). The observed In−In bond lengths in **1** and **2** are close to those observed in the binary compounds $SrIn_2$ and $SrIn_4$.[20] The In−Ge distances in **1** (2.751(1) Å) and **2** (2.780(2) Å) are comparable to those found in related polar intermetallic compounds containing In and Ge.[2,10a] Each Ge atom is 3-bonded to two neighboring Ge atoms and one indium atom, forming nominal zigzag chains of Ge atoms. The Ge−Ge distances in **1** and **2** are 2.522(1) and 2.557(2) Å, respectively. These are comparable to those found in hp-$BaGe_2$ (2.453 and 2.684 Å).[13a] The nominal Ge zigzag chains in **1** and **2** are very similar to those in hp-$BaGe_2$ ($ThSi_2$ type) in that the dihedral angles of the chains are 0°. However, closer inspection of the connectivity with the nominal In chains shows striking differences. The slight tilting of the Ge zigzag chains with respect to the *c*-axis (Ge−In bonds) results in a non-trigonal planar geometry about the Ge atoms, as shown in Figure 2b. The resulting Ge−Ge−Ge zigzag angles of 104.42(7)° and 104.59(9)° for **1** and **2**, respectively, are much smaller than the corresponding angles in $BaGe_2$, which are close to 120°. Thus, the pyramidalization of the germanium atoms in the zigzag chains indicates the onset of stereochemically active lone pairs and a significant decrease of the π-conjugation. In **1** and **2**, the cations (Eu and Sr) are located within nominal channels of 5-membered and 7-membered rings formed by the In−Ge network along *a*, as shown in Figure 2a. Each cation is 11-coordinated by six indium and five germanium atoms. The cations can also be viewed as being located within large channels of 12-membered rings formed by the In−Ge network along *b* (Figure 2b). The observed Eu−In, Eu−Ge, Sr−In, and Sr−Ge distances are comparable to those found in related strontium and europium polar intermetallic indides and germanides.[2,5,6,17a]

According to the Zintl−Klemm concept, EuInGe can be formulated as $Eu^{2+}(4b\text{-}In)^{-}(3b\text{-}Ge)^{-}$, and SrInGe as $Sr^{2+}(4b\text{-}In)^{-}(3b\text{-}Ge)^{-}$. Both ternary compounds EuInGe and SrInGe are Zintl phases. Formally, both Zintl compounds can be considered as a "one-electron oxidative-distortion" of the hp-$BaGe_2$ and LaAlGe which are isostructural with the tetragonal $ThSi_2$ and LaPtSi structures, respectively.[13b] The "one-electron deficiency" in **1** and **2**, with respect to the structures of the Zintl phases LaAlGe and hp-$BaGe_2$, is compensated by the formation of In−In bonds between neighboring parallel In chains, and the onset of stereochemically active lone pairs on the Ge atoms. The loss of the trigonal planar geometry around In and Ge in going from the $ThSi_2$ type to the EuInGe type indicates the loss of conjugation and the transformation of the π^* states to lone pairs on Ge and σ-bonding states between In. The In−In interchain bonding interaction also provides an effective rationale for the observed crystallographic disorder of the indium atoms: each In atom can have two possible directions in their approach to forming interchain bonds. All attempts to synthesize the Ba analogue were unsuccessful, resulting in the formation of BaGe and $BaIn_2$. The failures can be explained by the larger size of a Ba cation that leads to weaker interactions between neighboring indium chains. We also attribute the unsuccessful attempts to prepare BaInGe to the inherent thermodynamic stability of BaGe.[21]

To assess the chemical bonding of the new Zintl phases, three-dimensional band structures were calculated for the anionic $[InGe]^{2-}$ network in EuInGe. The calculations were performed on both ideal (In at the *m* sites) and distorted (disordered) models. The crystallographic disorder was

(20) (a) Iandelli, A. *Z. Anorg. Allg. Chem.* **1964**, *330*, 221. (b) Seo, D.-K.; Corbett, J. D. *J. Am. Chem. Soc.* **2000**, *122*, 9621.

(21) Goodey, J. Ph.D. Thesis, University of Houston, 2001.

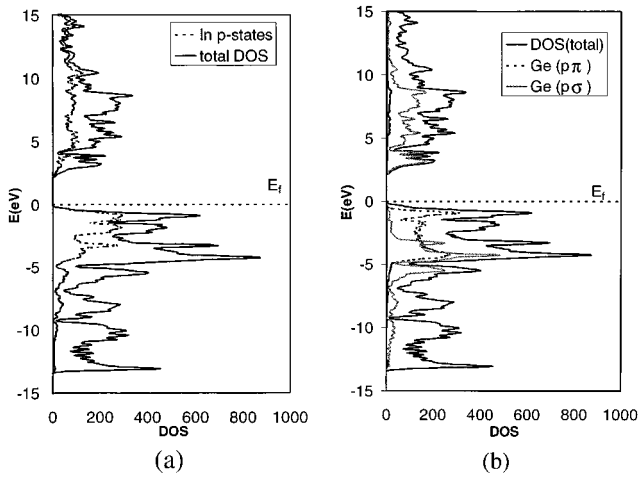

Figure 3. Relevant densities-of-states (DOS) curves for EuInGe: (a) projection of the contribution of In p states (dotted line) to the total density-of-states; and (b) projection of the contribution of Ge p_σ states and p_π states to the total density-of states (DOS). The Fermi level (E_F) is set to 0.0 eV.

addressed by using an ordered model with a doubled repetition length, with In alternately located on the two possible sites. Results of the calculations for the disordered structure are summarized in Figures 3 and 4. The density-of-states (DOS) diagram indicates that EuInGe is a semiconductor characterized by filled valence bands and a calculated band gap of 1.86 eV (Figure 3). The bands just below the Fermi level are mainly indium-derived p states, as well as the germanium-derived π^* states (lone pairs). These states immediately below the Fermi level represent In−In σ-bonding states and the weak antibonding states (In−Ge and Ge−Ge) associated with the germanium lone-pair states. Separate calculations on the ideal anionic $[InGe]^{2-}$ structure with indium atoms on the mirror plane (m) surprisingly indicate that the In−In interchain $p_\pi-p_\pi$ σ interactions are significantly bonding, with a summed overlap population of 0.14. Thus, a distortion leading to σ overlap between neighboring parallel chains of indium further increases the bonding overlap population, and the distorted structure is favored. Calculations on the actual distorted structure yield summed Mulliken overlap populations for the interchain and intrachain In−In interactions of 0.694 and 0.791, respectively. Further analysis of the overlap populations (COOP) indicates that all In−In bonding interactions, including the long "interchain" (3.170 Å) bonds, are optimized at the Fermi level. This indicates that indeed the In atoms in EuInGe are 4-bonded and their oxidation state is equivalent to $[In]^-$.

In the ordered $ThSi_2$ model of the $[InGe]^{2-}$ anionic network, the germanium π^* states are occupied and each Ge is in full conjugation with its two Ge neighbors. However, calculations on the ideal ($ThSi_2$) and distorted models of EuInGe show that upon distortion the Ge p_{π^*} orbitals are localized as lone pairs perpendicular to the c-axis. Thus, the pyramidal geometry of each Ge atom represents the onset of a stereochemically active lone pair that provides the stabilization of the filled π^* states. In electron-rich compounds with 3-connected anionic nets, as in $ThSi_2$, the restriction of the π^* dispersion along the chains has been noted to be a stabilizing factor to their chemical bonding.[7] The electronic band structure calculations also confirm that the 3-bonded Ge atoms are equivalent to $[Ge]^-$. The assigned oxidation states in EuInGe are in agreement with the calculated charge populations of −1.3 and −0.7 for Ge and In, respectively. The conduction bands just above the Fermi level are mainly derived from the Ge p_σ orbitals of the Ge chain with minor contributions from the indium p states. These conduction states represent mainly antibonding interactions, along the Ge chain, as well as indium interactions between parallel indium zigzag chains. The crystal overlap population curves (COOP), as shown in Figure 4, summarize the relevant interactions in EuInGe.

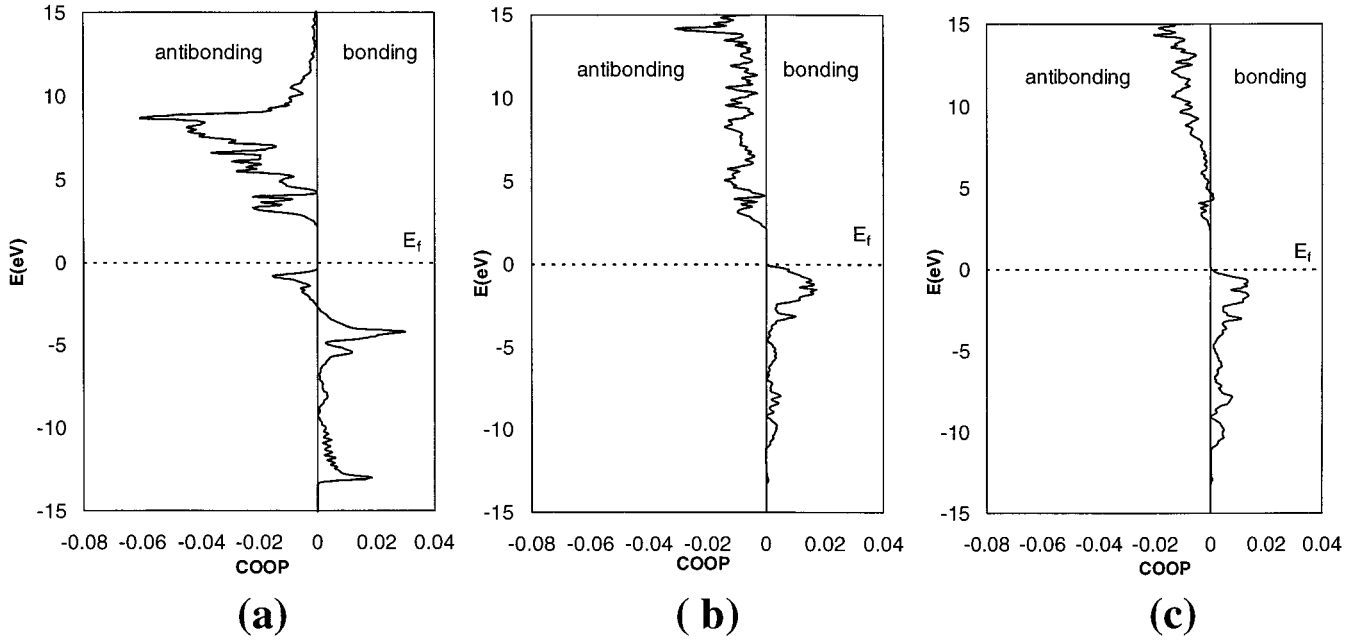

Figure 4. Crystal orbital overlap population (COOP) curves of EuInGe: (a) Ge−Ge bonds; (b) "interchain" In−In bonds; and (c) average overlap population of intrachain In−In bonds. The Fermi level (E_F) is set to 0.0 eV.

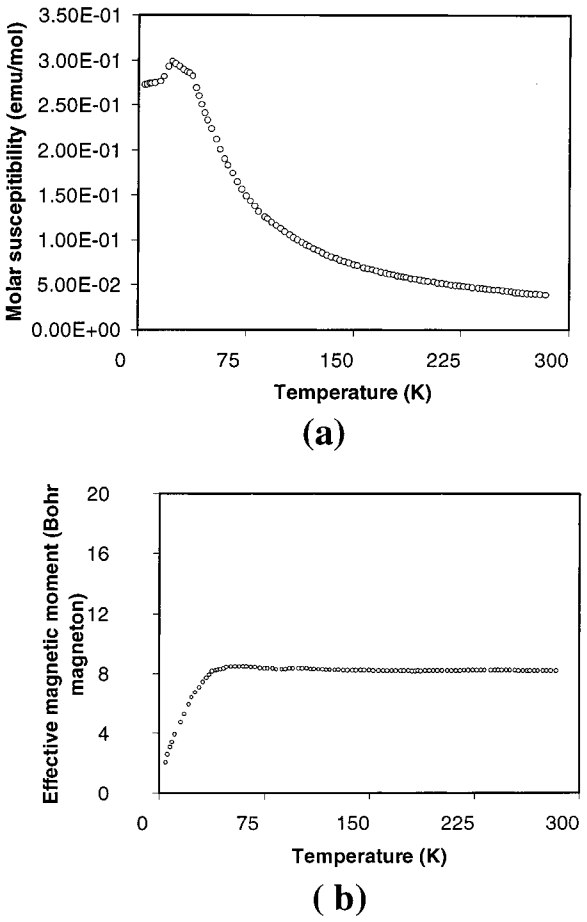

Figure 5. Magnetic property measurements for EuInGe: (a) plot of the molar susceptibility (χ_m) of EuInGe as a function of temperature (T); and (b) plot of the effective magnetic moments (μ_{eff}) of EuInGe as a function of temperature (T).

Owing to the interesting magnetic properties exhibited by many Eu compounds, the magnetic behavior of EuInGe was measured on single-phase powder samples at a temperature range between 4 and 300 K. After relevant corrections were made, magnetic susceptibility measurements indicated that EuInGe exhibits Curie−Weiss paramagnetic behavior above 35 K, as shown in Figure 5. The effective magnetic moments were calculated from the slope of the χ^{-1}-vs-T data at a constant field of 0.5 T (Figure 5b). This yields an effective paramagnetic moment, $\mu_{eff} = 8.11\ \mu_B$, between 35 and 300 K. The calculated μ_{eff} agrees well with the expected free-ion value for Eu^{2+} of 7.94 μ_B obtained from the relation $\mu_{eff} = g[J(J + 1)]^{1/2}\mu_B$.[22] The paramagnetic compound EuInGe orders antiferromagnetically below 35 K (Figure 5a), shown as a cusp at 35 K in the χ-vs-T plot, and its μ_{eff} value decreases to 2.1 μ_B at 4 K. The antiferromagnetic behavior of EuInGe is similar to that exhibited by similar europium aluminides, $EuAl_2$ and $EuAl_4$, as well as in $EuSi_2$.[19] Moreover, the Neel temperature of $EuSi_2$ ($T_N = 39$ K) that crystallizes in the tetragonal $ThSi_2$ structure is slightly higher than the corresponding transition temperature for EuInGe ($T_N = 35$ K). Similar magnetic measurements on SrInGe indicate that the compound is diamagnetic. Thus, the magnetic behaviors of EuInGe and SrInGe confirm the divalent state for Eu(II) and Sr(II) and support the oxidation assignments in accordance with the Zintl concept: $Eu^{2+}[In^-Ge^-]$ and $Sr^{2+}[In^-Ge^-]$.

Acknowledgment. This work is supported by the National Science Foundation (CAREER Award, DMR-9733587), the Texas Center for Superconductivity at the University of Houston, and the Petroleum Research Fund administered by the American Chemical Society. This work made use of MRSEC/TCSUH Shared Experimental Facilities supported by the NSF (DMR-9632667) and the State of Texas through the TCSUH.

Supporting Information Available: Two X-ray crystallographic files, in CIF format. This material is available free of charge via the Internet at http://pubs.acs.org.

IC0102891

(22) (a) Labroo, S.; Ali, N. *J. Appl. Phys.* **1990**, *67*, 4811. (b) Ernet, U.; Müllmann, R.; Mosel, B. D.; Eckert, H.; Pöttgen, R.; Kotzyba, G. *J. Mater. Chem.* **1997**, *7*, 255.
(23) Mader, K. H.; Wallace, W. E. *J. Chem. Phys.* **1968**, *49*, 1521.